Estimating Mean Profiles and Fluxes in High-Speed Turbulent Boundary Layers Using Inner/Outer-Layer Scalings

Hasan, Asif Manzoor; Larsson, Johan; Pirozzoli, Sergio; Pecnik, Rene

DOI
10.2514/1.J063335

Publication date
2024

Document Version
Final published version

Published in
AIAA Journal

AIAA JOURNAL
Vol. 62, No. 2, February 2024

Technical Notes

Estimating Mean Profiles and Fluxes in High-Speed Turbulent Boundary Layers Using Inner/Outer-Layer Scalings

Asif Manzoor Hasan*
Delft University of Technology, 2628 CB Delft, The Netherlands
Johan Larsson†
University of Maryland, College Park, Maryland 20742
Sergio Pirozzoli‡
Sapienza University of Rome, 00184 Rome, Italy
and
Rene Pecnik§
Delft University of Technology, 2628 CB Delft, The Netherlands

https://doi.org/10.2514/1.J063335

Nomenclature

C = log-law intercept
c_f = skin-friction coefficient, $2\tau_w/(\rho_\infty u_\infty^2)$
c_h = heat-transfer coefficient, $q_w/(c_p\rho_\infty u_\infty(T_w - T_r))$
c_p = specific heat capacity at constant pressure
k = thermal conductivity
M_τ = friction Mach number, $u_\tau/\sqrt{\gamma RT_w}$
M_∞ = freestream Mach number, $u_\infty/\sqrt{\gamma RT_\infty}$
Pr = Prandtl number, $\mu c_p/k$
q_w = wall heat flux
R = specific gas constant
Re_{δ^*} = displacement thickness Reynolds number, $\rho_\infty u_\infty \delta^*/\mu_\infty$
Re_{δ_2} = momentum thickness Reynolds number with viscosity at the wall, $\rho_\infty u_\infty \theta/\mu_w$
Re_θ = momentum thickness Reynolds number, $\rho_\infty u_\infty \theta/\mu_\infty$
Re_τ = friction Reynolds number, $\rho_w u_\tau \delta/\mu_w$
Re_τ^* = semilocal friction Reynolds number, $\bar{\rho} u_\tau^* \delta/\bar{\mu}$
r = recovery factor
T = temperature
u = mean velocity
u_τ = friction velocity at the wall, $\sqrt{\tau_w/\rho_w}$
u_τ^* = semilocal friction velocity, $\sqrt{\tau_w/\bar{\rho}}$
y = wall-normal coordinate
y^* = semilocal wall-normal coordinate, y/δ_v^*
γ = specific heat capacity ratio
δ = (or δ_{99}), boundary-layer thickness
δ_v = viscous length scale at the wall, $\mu_w/(\rho_w u_\tau)$
δ^* = displacement thickness
δ_v^* = semilocal viscous length scale, $\bar{\mu}/(\bar{\rho} u_\tau^*)$
θ = momentum thickness
κ = von Kármán constant
μ = dynamic viscosity
μ_t = eddy viscosity
Π = Coles's wake parameter
ρ = density
τ_w = wall shear stress

Subscripts

e = boundary-layer edge ($y = \delta$)
r = recovery
w = wall
∞ = freestream

Superscripts

$+$ = wall-scaled
$\overline{(\cdot)}$ = Reynolds averaging

Received 30 June 2023; revision received 24 October 2023; accepted for publication 24 October 2023; published online Open Access 30 November 2023.

*Ph.D. Candidate, Process and Energy Department, Leeghwaterstraat 39; a.m.hasan@tudelft.nl (Corresponding Author).
†Professor, Department of Mechanical Engineering. Associate Fellow AIAA.
‡Professor, Department of Mechanical and Aerospace Engineering, Via Eudossiana 18.
§Professor, Process and Energy Department, Leeghwaterstraat 39; r.pecnik@tudelft.nl (Co-Corresponding Author).

I. Introduction

ACCURATELY predicting drag and heat transfer for compressible high-speed flows is of utmost importance for a range of engineering applications. A common approach is to use a compressible velocity scaling law (transformation) that inverse-transforms the velocity profile of an incompressible flow, coupled with a temperature–velocity relation. Current methods [1,2] typically assume a single velocity scaling law, overlooking the different scaling characteristics of the inner and outer layers. In this Note, we use distinct velocity scalings for these two regions and model the velocity profile for compressible boundary layers using a classic eddy viscosity expression combined with a defect law. The inner-layer velocity profile is modeled using the mixing-length eddy viscosity from Hasan et al. [3], which incorporates variable property effects through semilocal scaling and accounts for intrinsic compressibility effects by adjusting the near-wall damping function. The outer-layer profile is modeled after Coles's law of the wake [4], scaled according to the Van Driest (VD) velocity scaling [5]. The result is an analytical expression for the mean shear valid in the entire boundary layer, which, combined with the temperature–velocity relationship from Zhang et al. [6], provides predictions of mean velocity and temperature profiles at high accuracy. Using these profiles, drag and heat-transfer coefficients are evaluated with an accuracy of ±4 and ±8%, respectively, for a wide range of zero pressure gradient compressible turbulent boundary layers up to Mach numbers of 14.

II. Proposed Method

The velocity profile of a turbulent boundary layer is composed of two parts: 1) the law of the wall in the inner layer, and 2) the velocity defect law in the outer layer. Using an eddy viscosity model for the inner layer and Coles's law of the wake for the outer layer, the mean shear for incompressible flows can be expressed as

$$\frac{d\bar{u}_{\text{inc}}}{dy} = \frac{u_\tau}{\delta_v}\frac{1}{1+\mu_t/\mu_w} + \frac{u_\tau}{\delta}\frac{\Pi}{\kappa}\pi\sin\left(\pi\frac{y}{\delta}\right) \tag{1}$$

where the first term on the right-hand side can be readily obtained by integrating the mean momentum equation (stress balance) of equilibrium flows, while the second term is the derivative of Coles's wake

function [7]. Modeling μ_t using simple inner-layer mixing-length models would lead to a linear profile close to the wall, developing into a logarithmic profile that extends to the outer layer, where it is added to the wake component, as desired.

In compressible flows, the stress balance equation in the inner layer leads to the mean shear given by $d\bar{u}/dy = (u_\tau^*/\delta_v^*)/(1 + \mu_t/\bar{\mu})$ [3]. For the wake region, following Van Driest's velocity scaling, u_τ is replaced with u_τ^* to account for mean density variations while maintaining the same outer-layer length scale, δ [8]. With these changes, the mean shear for compressible flows reads

$$\frac{d\bar{u}}{dy} = \frac{u_\tau^*}{\delta_v^*}\frac{1}{1+\mu_t/\bar{\mu}} + \frac{u_\tau^*}{\delta}\frac{\Pi}{\kappa}\pi\sin\left(\pi\frac{y}{\delta}\right) \tag{2}$$

Now, modeling $\mu_t/\bar{\mu}$ based on the Johnson–King (JK) mixing-length eddy viscosity model [9], corrected for variable property and intrinsic compressibility effects [3], we get

$$\frac{d\bar{u}}{dy} = \frac{u_\tau^*}{\delta_v^*}\frac{1}{1+\kappa y^* D(y^*, M_\tau)} + \frac{u_\tau^*}{\delta}\frac{\Pi}{\kappa}\pi\sin\left(\pi\frac{y}{\delta}\right) \tag{3}$$

Equation (3) provides several useful insights. Analogous to an incompressible flow, the mean velocity in a compressible flow is controlled by two distinct length scales, δ_v^* and δ, characteristic of the inner and outer layers, respectively. The two layers are connected by a common velocity scale u_τ^* (the semilocal friction velocity), leading to a logarithmic law in the overlap region. Moreover, in the logarithmic layer and beyond, the first term on the right-hand side reduces to $\sqrt{\tau_w/\bar{\rho}}/(\kappa y)$, which is consistent with Van Driest's original arguments [5]. It is crucial to satisfy this condition; otherwise, the logarithmic profile extending to the outer layer would not obey Van Driest's scaling, while the wake component to which it is added would.

The near-wall damping function in Eq. (3) is given by

$$D(y^*, M_\tau) = \left[1 - \exp\left(\frac{-y^*}{A^+ + f(M_\tau)}\right)\right]^2 \tag{4}$$

The value of A^+ differs based on the choice of the von Kármán constant κ, such that the log-law intercept is reproduced for that κ [10]. With $\kappa = 0.41$, the value of $A^+ = 17$ gives a log-law intercept of 5.2 [11], whereas, with $\kappa = 0.384$, $A^+ = 15.22$ gives a log-law intercept of 4.17. The additive term $f(M_\tau)$ accounts for intrinsic compressibility effects. Hasan et al. [3] proposed $f(M_\tau) = 19.3M_\tau$, which is independent of the chosen value of κ.

The second term on the right-hand side of Eq. (3) is the wake term accounting for mean density variations, where Coles's wake parameter Π depends on the Reynolds number, as discussed in the subsection below. It is important to note that Π also depends on pressure gradient [4]; however, the focus of the current analysis is limited to zero pressure gradient turbulent boundary layers.

A. Characterizing Low-Reynolds-Number Effects on the Wake Parameter

For incompressible boundary layers, Coles's wake parameter is known to strongly depend on Re_θ at low Reynolds numbers [12–14]. For compressible boundary layers, the ambiguity of the optimal Reynolds number definition poses a challenge to characterize the wake parameter. Fernholz and Finley [15], mainly using experimental data at that time, observed that the momentum thickness Reynolds number with viscosity at the wall (Re_{δ_2}) is the suitable definition to scale Π. On the other hand, Wenzel et al. [16] observed that the wake parameter scales with Re_θ for their direct numerical simulations (DNSs) at moderate Mach numbers ($M_\infty \leq 2.5$), consistent with the expectation that Π (being defined at the boundary-layer edge) should scale with Reynolds number based on the freestream properties [8,14]. Yet, there is no clear consensus on which definition is relevant in scaling Π, especially for high-Mach-number flows, where Re_{δ_2} and Re_θ are quite different from each other. Given the recent availability of hypersonic DNS, we revisit the question of which Reynolds number best describes the wake parameter.

First, we evaluate Π for several incompressible and compressible DNS cases from the literature and then report it as a function of different definitions of the Reynolds number, searching for the definition yielding the least spread of the data points. For incompressible flows, the wake strength can be determined as $\Pi = 0.5\kappa(\bar{U}^+(y=\delta) - (1/\kappa)\,\ell_n(\delta^+) - C)$, where C is the log-law intercept for the chosen κ. For compressible flows, the wake strength is based on the VD-transformed velocity [8,15] as $\Pi = 0.5\kappa(\bar{U}_{\mathrm{vd}}^+(y=\delta) - (\bar{U}_{\mathrm{vd}}^+)^{\log}(y=\delta))$, where $\bar{U}_{\mathrm{vd}}^+$ is obtained from the DNS data. The reference log law $(\bar{U}_{\mathrm{vd}}^+)^{\log}$, unlike for incompressible flows, cannot be computed as $(1/\kappa)\,\ell_n(y^+) + C_{\mathrm{vd}}$, because C_{vd} is found to be nonuniversal for diabatic compressible boundary layers [17,18]. Hence, $(\bar{U}_{\mathrm{vd}}^+)^{\log}$ can be obtained either by fitting a logarithmic curve to $\bar{U}_{\mathrm{vd}}^+$ [15], or by inverse-transforming the incompressible law of the wall. Here, we follow the latter approach by using the compressibility transformation of Hasan et al. [3].

The value of the von Kármán constant κ plays a crucial role in estimating Π. Spalart [19] noted that a strong consensus on κ is needed to accurately estimate Π. However, such a consensus is yet missing [20]. Nagib and Chauhan [10] showed that $\kappa = 0.384$ is a suitable choice for incompressible boundary layers, verified to be true also for channels [21] and pipes [22]. However, due to historical reasons and wide acceptance of $\kappa = 0.41$, we will proceed with this value. The same procedure can straightforwardly be repeated with a different value of κ.

Figure 1 shows the wake parameter for 26 compressible and nineteen incompressible boundary-layer flows, as a function of Re_{δ_2}, Re_θ, Re_{δ^*}, and $Re_{\tau_\infty}^*$. The spread in the data points is found to be quite large for all the definitions, as Π is the difference of two relatively large quantities, namely, $\bar{U}_{\mathrm{vd}}^+$ and $(\bar{U}_{\mathrm{vd}}^+)^{\log}$, at the boundary-layer edge, as outlined above. Note that even incompressible boundary layers are not devoid of this scatter [13,19]. Figure 1a shows the presence of two distinct branches; hence, Re_{δ_2} does not seem to be suitable to characterize Π, unlike reported in previous literature [1,15]. Among the four definitions of Reynolds number, Re_θ seems to show the least spread, further confirming the conclusions in Wenzel et al. [16]. Figure 1b also reports several functional forms of $\Pi = f(Re_\theta)$. Use of the modified Kármán–Schoenherr friction formula [31] for indirect evaluation of Π does not show saturation at high Reynolds numbers as observed by Coles [12] for incompressible flows. The Cebeci–Smith (hereafter CS) relation [14] underpredicts Π but reproduces saturation at high Reynolds numbers. Wenzel et al. [16] modified the CS relation with a higher saturation value of Π (0.66) and fit it to the DNS data of Schlatter et al. [23] and Schlatter and Orlu [24]. Here, we propose a relation similar to that proposed by [14], but fitted to the more recent incompressible DNS data of Jiménez et al. [25] and Sillero et al. [26], in which particular care was exercised to guarantee that the numerical boundary layers are in a fully developed state. Those data support similar behavior as CS in the low-Re regime, but with a higher saturation value, resulting in the relation

$$\Pi = 0.69[1 - \exp(-0.243\sqrt{z} - 0.15z)], \quad \text{where } z = Re_\theta/425 - 1 \tag{5}$$

We also note that some high-Reynolds-number cases have a higher value of the wake parameter than that predicted by Eq. (5). This could be due to the previously noted high data scatter or to inaccuracies arising from the application of the Van Driest transformation to the wake velocity profile, or both. Regardless, these differences are tolerable for the scope of the present paper, as the results are not highly sensitive to the precise value of the wake parameter (see Sec. III).

The inset in Fig. 1b compares the skin-friction curve computed using Eq. (5) with the modified Kármán–Schoenherr skin-friction formula [31]. The distance between the two curves is large at low Reynolds numbers but less so at higher Reynolds numbers.

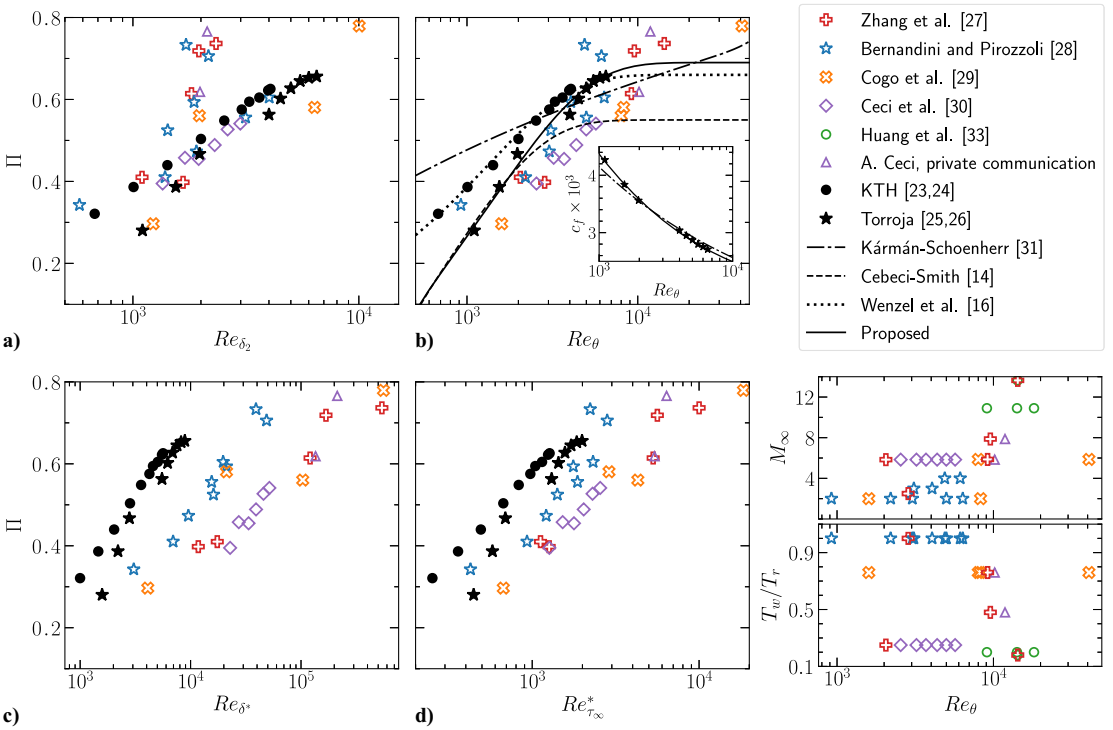

Fig. 1 The wake parameter Π computed using the DNS data and plotted as a function of a) Re_{δ_2}, b) Re_θ, c) Re_{δ^*}, and d) $Re^*_{\tau_\infty}$ for 19 incompressible [23–26] and 26 compressible ([27–30] and A. Ceci [Ph.D. student, Sapienza University of Rome], private communication) turbulent boundary layers.

As expected, the incompressible DNS data of Jiménez et al. [25] and Sillero et al. [26] follow the friction curve computed using Eq. (5).

B. Implementation of the Proposed Method

For convenience of implementation, Eq. (3) can also be expressed in terms of the dimensional quantities τ_w, $\bar{\mu}$, and $\bar{\rho}$ as

$$\frac{d\bar{u}}{dy} = \frac{\tau_w}{\bar{\mu} + \underbrace{\sqrt{\tau_w\bar{\rho}}\kappa y D(y^*, M_\tau)}_{\mu_t}} + \frac{\sqrt{\tau_w/\bar{\rho}}}{\delta}\frac{\Pi}{\kappa}\pi\sin\left(\pi\frac{y}{\delta}\right) \tag{6}$$

where μ_t is the dimensional form of the JK eddy viscosity model, which can be readily used in turbulence modeling, for instance, as a wall model in large-eddy simulations (LESs). Note that other eddy viscosity models can also be used in Eq. (6), e.g., Prandtl's mixing-length model (see Appendix A).

Equation (6) covers the entire boundary layer, and it can be integrated in conjunction with a suitable temperature model such as the one proposed by Zhang et al. [6], which is given as

$$\frac{\bar{T}}{T_w} = 1 + \frac{T_r - T_w}{T_w}\left[\left(1 - s\ Pr\right)\left(\frac{\bar{u}}{u_\infty}\right)^2 + s\ Pr\left(\frac{\bar{u}}{u_\infty}\right)\right] + \frac{T_\infty - T_r}{T_w}\left(\frac{\bar{u}}{u_\infty}\right)^2 \tag{7}$$

where $s\ Pr = 0.8$, $T_r/T_\infty = 1 + 0.5r(\gamma-1)M_\infty^2$, and $r = Pr^{1/3}$. Moreover, a suitable viscosity law (e.g., power or Sutherland's law) and the ideal gas equation of state $\bar{\rho}/\rho_w = T_w/\bar{T}$ have to be used to compute mean viscosity and density profiles, respectively. The inputs that need to be provided are the Reynolds number Re_θ, free-stream Mach number M_∞, wall cooling/heating parameter T_w/T_r, and (optionally) the dimensional wall or freestream temperature for Sutherland's law. It is important to note that Eq. (7) and all solver inputs are based on the quantities in the freestream and not at the boundary-layer edge. For more insights on the solver, refer to the source code available on GitHub [32].

III. Results

Figure 2 shows the predicted velocity and temperature profiles for a selection of high-Mach-number cases. As can be seen, the DNS and the predicted profiles are in good agreement, thus corroborating our methodology. The insets in Fig. 2 show the error in the predicted skin-friction and heat-transfer coefficients for 30 compressible cases from the literature. For most cases, the friction coefficient c_f is predicted with ±4% accuracy, with a maximum error of −5.3%. The prediction of the heat-transfer coefficient c_h shows a slightly larger error compared to c_f, potentially due to additional inaccuracies arising from the temperature–velocity relation. In most cases, c_h is predicted with ±8% accuracy, with a maximum error of 10.3%.

To assess the sensitivity of the predictions with respect to the relation used for the wake parameter, we recomputed the results using our method, but instead of using Eq. (5) to estimate Π, we employed the relation proposed by Wenzel et al. [16]. The maximum error in the c_f prediction changed from −5.3 to −6.08%, with most of the cases within error bounds of ±5%. For the c_h prediction, there was an increase in the maximum error from 10.3 to 11.4%, with most of the cases within error bounds of ±8%.

Instead of using the eddy-viscosity-based mean shear equation (6), the mean velocity profile can also be obtained based on inverse velocity transformations applied to the reference incompressible profile. Here, instead of using a single transformation for the entire boundary layer [1,2], we rather advocate the use of distinct transformations for the inner and outer layers. Considering the reference incompressible velocity profile as being made up of the sum of an inner part ($\bar{U}^+_{\text{inn}}$) and of a wake correction ($\bar{U}^+_{\text{wake}}$), we separately inverse-transform the related velocity increments to yield

$$d\bar{u}^+ = \mathcal{T}^{-1}_{\text{inn}} d\bar{U}^+_{\text{inn}} + \mathcal{T}^{-1}_{\text{out}} d\bar{U}^+_{\text{wake}} \tag{8}$$

where $\mathcal{T}_{\text{inn}}$ and $\mathcal{T}_{\text{out}}$ denote the inner- and outer-layer velocity transformation kernels, respectively. Employing the transformation kernels of Hasan et al. [3] and Van Driest [5] for $\mathcal{T}_{\text{inn}}$ and $\mathcal{T}_{\text{out}}$, respectively, and modeling $\bar{U}^+_{\text{inn}}$ using the JK model and $\bar{U}^+_{\text{wake}}$ from Coles's law of the wake, one can readily arrive at the mean shear equation (6) (see Appendix B). The advantage of using Eq. (8) is

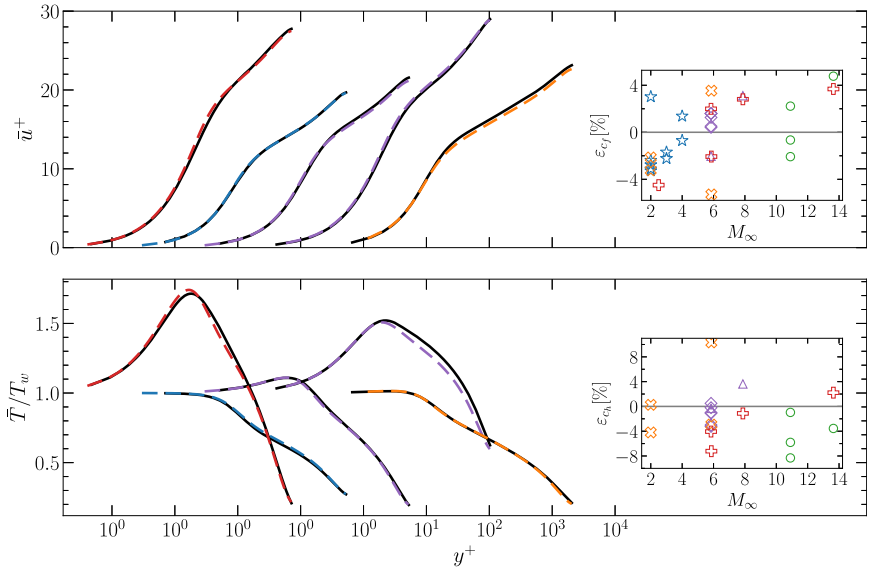

Fig. 2 Predicted velocity (top) and temperature (bottom) profiles (dashed lines) compared to DNS (black solid lines) for the cases with the highest reported Mach numbers in the respective publications: *Left to right:* $M_\infty = 13.64$, $T_w/T_r = 0.18$ [27]; $M_\infty = 4$, $T_w/T_r = 1$ [28]; $M_\infty = 7.87$, $T_w/T_r = 0.48$ (A. Ceci [Ph.D. student, Sapienza University of Rome], private communication); $M_\infty = 5.84$, $T_w/T_r = 0.25$ [30];$M_\infty = 5.86 T_w/T_r = 0.76$ [29]. *Insets:* Percent error in skin-friction (top) and heat-transfer (bottom) predictions for 30 compressible turbulent boundary layers from the literature ([27–30,33] and A. Ceci [Ph.D. student, Sapienza University of Rome], private communication). The error is computed as $\varepsilon_{c_f} = (c_f - c_f^{\mathrm{DNS}})/c_f^{\mathrm{DNS}} \times 100$ and likewise for ε_{c_h}. Symbols are as in Fig. 1.

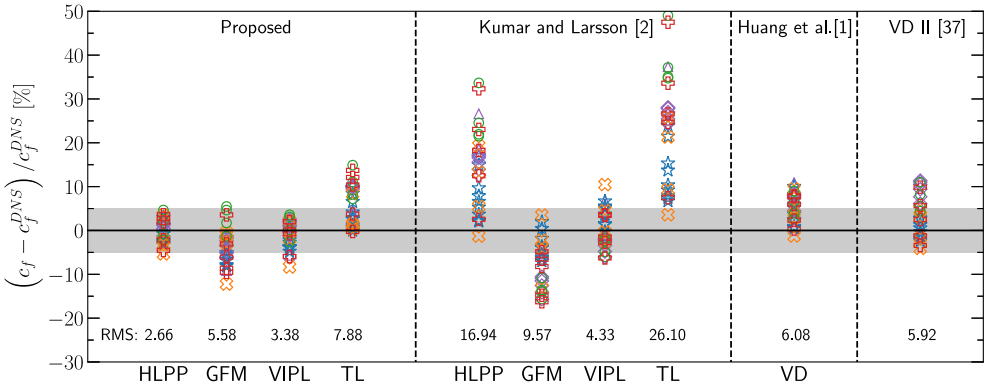

Fig. 3 Error in skin-friction prediction using the proposed approach compared to different state-of-the-art approaches. The letters on the X axis denote the velocity transformation used for that approach. HLPP, GFM, VIPL, TL, and VD stand for the transformations proposed by Hasan et al. [3], Griffin et al. [34], Volpiani et al. [35], Trettel and Larsson [18], and Van Driest [5], respectively. The numbers are RMS values computed as outlined in the text. Symbols are as in Fig. 1. The shaded region shows an error bar of ±5%. Note that inputs for all the methods are based on properties in the freestream instead of at the edge of the boundary layer.

that it makes the proposed method modular, as it can also be applied using other velocity transformations as building blocks [18,34–36], although with minor modifications, as discussed in Appendix C. This is shown in Fig. 3, which compares the proposed approach with the modular approach of Kumar and Larsson [2], both with different inner-layer transformations. Additionally, the figure includes results obtained with the method of Huang et al. [1] using the VD transformation and the widely recognized Van Driest II skin-friction formula [37]. Figure 3 also shows the root-mean-square error, determined as $\mathrm{RMS} = \sqrt{(1/N)\sum \varepsilon_{c_f}^2}$, where N is the total number of DNS cases considered. The Van Driest II formula and the method of Huang et al. have similar RMS error of about 6%,[¶] which is not surprising as both of them are built on Van Driest's mixing-length arguments. The errors are systematically positive for a majority of the cases and increase with a higher Mach number and stronger wall cooling. The source of this error mainly resides in the inaccuracy of the VD velocity transformation in the near-wall region for diabatic flows. To eliminate this shortcoming, Kumar and Larsson [2] developed a modular methodology, which is quite accurate when the transformation of Volpiani et al. [35] is used but is less accurate if other velocity transformations are implemented. This inaccuracy is because the outer-layer velocity profile is also inverse-transformed according to the inner-layer transformation. In the current approach, the velocity profile is instead inverse-transformed using two distinct transformations that take into account the different scaling properties of the inner and outer layers, thus reducing the RMS error with respect to Kumar and Larsson's modular method for all the transformations tested herein. The error using the proposed approach with the TL transformation is positive for all the cases. This is due to the log-law shift observed in the TL scaling, which is effectively removed in the Hasan et al. [3] transformation, thereby yielding an RMS error of 2.66%, which is the lowest among all approaches.

IV. Conclusions

We have derived an expression for the mean-velocity gradient in high-speed boundary layers [Eq. (6)] that uses distinct velocity scalings in the inner [3] and outer [5] layers, thus covering the entire boundary layer. Coles's wake parameter in this expression is

[¶]Huang et al.'s method with the more accurate temperature velocity relation in Ref. [6] leads to an RMS error of 12%.

determined using an adjusted Cebeci and Smith relation [Eq. (5)], with Re_θ found to be the most suitable parameter to characterize low-Reynolds-number effects on Π. This method allows remarkably accurate predictions of the mean velocity and temperature profiles, leading to estimations of the friction and heat-transfer coefficients that are within ± 4 and $\pm 8\%$ of the DNS data, respectively. When compared with other skin-friction prediction methods in the literature, our approach yields the lowest RMS error of 2.66%.

The methodology developed in this Note promises straightforward application to other classes of wall-bounded flows like channels and pipes upon change of the temperature–velocity relation (e.g., [38]) and using different values of the wake parameter Π [10]. Also, the method is modular in the sense that it can be used with other temperature models and equations of state.

Appendix A: Mean Shear Using Prandtl's Mixing-Length Model

The choice of the eddy viscosity model affects the first term on the right-hand side of Eq. (6). By analogy, the mean shear equation using Prandtl's mixing-length model is thus as follows:

$$\frac{d\bar{u}}{dy} = \frac{2\tau_w}{\bar{\mu} + \sqrt{\bar{\mu}^2 + [2\sqrt{\tau_w \bar{\rho}}\kappa y D(y^*, M_\tau)]^2}} + \frac{\sqrt{\tau_w/\bar{\rho}}}{\delta}\frac{\Pi}{\kappa}\pi \sin\left(\pi \frac{y}{\delta}\right) \tag{A1}$$

where $D(y^*, M_\tau)$ is the damping function, corrected for intrinsic compressibility effects as

$$D(y^*, M_\tau) = 1 - \exp\left(\frac{-y^*}{A^+ + 39M_\tau}\right) \tag{A2}$$

with $A^+ = 25.53$ (or 26) for $\kappa = 0.41$, and where the additive term $39M_\tau$ is obtained following similar steps as for the JK model (see Ref. [3]).

Appendix B: Deriving the Mean Shear Equation Using Velocity Transformations

Starting from Eq. (8) and using Hasan et al. [3] and Van Driest [5] transformation kernels, we get

$$d\bar{u}^+ = f_3^{-1} f_2^{-1} f_1^{-1} d\bar{U}^+_{\text{inn}} + f_1^{-1} d\bar{U}^+_{\text{wake}} \tag{B1}$$

where the factors f_1, f_2, and f_3 are given by

$$f_1 = \sqrt{\frac{\bar{\rho}}{\rho_w}}, \quad f_2 = \left(1 - \frac{y}{\delta_v^*}\frac{d\delta_v^*}{dy}\right), \quad f_3 = \left(\frac{1 + \kappa y^* D(y^*, M_\tau)}{1 + \kappa Y^+ D(Y^+, 0)}\right) \tag{B2}$$

and the damping function $D(y^*, M_\tau)$ is as per Eq. (4). Here, Y denotes the wall-normal coordinate for the incompressible flow. In Eq. (B1), $d\bar{U}^+_{\text{inn}}$ is modeled using the JK eddy viscosity model as $dY^+/[1 + \kappa Y^+ D(Y^+, 0)]$, which, after integration, recovers the incompressible law of the wall, and $d\bar{U}^+_{\text{wake}} = (\Pi/\kappa)\sin(\pi Y/\delta)\pi d(Y/\delta)$ is the derivative of the Coles's wake function. Inserting the expressions for $d\bar{U}^+_{\text{inn}}$, $d\bar{U}^+_{\text{wake}}$ in Eq. (B1), we get

$$d\bar{u}^+ = f_3^{-1} f_2^{-1} f_1^{-1} \frac{dY^+}{1 + \kappa Y^+ D(Y^+, 0)} + f_1^{-1}\frac{\Pi}{\kappa}\pi \sin\left(\pi \frac{Y}{\delta}\right) d\left(\frac{Y}{\delta}\right) \tag{B3}$$

Now, using the inner- and outer-layer coordinate transformations as $Y^+ = y^*$ [3,18] and $Y = y$, respectively, and using $dY^+/dy = f_2/\delta_v^*$, $u_\tau = u_\tau^* f_1$, we get the dimensional form of the mean-velocity gradient as

$$\frac{d\bar{u}}{dy} = \frac{u_\tau^*}{\delta_v^*}\frac{1}{1 + \kappa y^* D(y^*, M_\tau)} + \frac{u_\tau^*}{\delta}\frac{\Pi}{\kappa}\pi \sin\left(\pi \frac{y}{\delta}\right) \tag{B4}$$

which is the same as Eq. (3) and subsequently leads to Eq. (6).

Appendix C: Implementation of the Method Using Velocity Transformations in Refs. [34,35]

Implementing Eq. (8) with the transformations in Volpiani et al. [35] and Griffin et al. [34] needs minor modification because the logarithmic profile extending to the outer layer, computed by their inverse, does not satisfy Van Driest's scaling, which is crucial as outlined in Sec. II. To address this issue, we enforce the Van Driest transformation in the outer layer by modifying Eq. (8) as follows:

$$\begin{aligned} Y^+ \le 50 &: d\bar{u}^+ = \mathcal{T}^{-1}_{\text{inn}} d\bar{U}^+_{\text{inn}}, \\ Y^+ > 50 &: d\bar{u}^+ = \mathcal{T}^{-1}_{\text{vd}} d\bar{U}^+_{\text{inn}} + \mathcal{T}^{-1}_{\text{vd}} d\bar{U}^+_{\text{wake}} \end{aligned} \tag{C1}$$

where $\mathcal{T}_{\text{inn}}$ and $\mathcal{T}_{\text{vd}}$ denote the inner-layer and Van Driest transformation kernels, respectively, and Y^+ is the transformed coordinate. The value of 50 is taken arbitrarily as the start of the logarithmic region.

Acknowledgments

We thank P. Costa for the insightful discussions. This work was supported by the European Research Council grant no. ERC-2019-CoG-864660, Critical; the Air Force Office of Scientific Research under grants FA-9550-23-1-0228 and FA8655-23-1-7016; and the Office of Naval Research under grant N00014-23-1-2459.

References

[1] Huang, P., Bradshaw, P., and Coakley, T., "Skin Friction and Velocity Profile Family for Compressible Turbulent Boundary Layers," *AIAA Journal*, Vol. 31, No. 9, 1993, pp. 1600–1604. https://doi.org/10.2514/3.11820

[2] Kumar, V., and Larsson, J., "Modular Method for Estimation of Velocity and Temperature Profiles in High-Speed Boundary Layers," *AIAA Journal*, Vol. 60, No. 9, 2022, pp. 5165–5172. https://doi.org/10.2514/1.J061735

[3] Hasan, A. M., Larsson, J., Pirozzoli, S., and Pecnik, R., "Incorporating Intrinsic Compressibility Effects in Velocity Transformations for Wall-Bounded Turbulent Flows," *Physical Review Fluids*, Vol. 8, No. 11, Nov. 2023, Paper L112601. https://doi.org/10.1103/PhysRevFluids.8.L112601

[4] Coles, D., "The Law of the Wake in the Turbulent Boundary Layer," *Journal of Fluid Mechanics*, Vol. 1, No. 2, 1956, pp. 191–226. https://doi.org/10.1017/S0022112056000135

[5] Van Driest, E. R., "Turbulent Boundary Layer in Compressible Fluids," *Journal of the Aeronautical Sciences*, Vol. 18, No. 3, 1951, pp. 145–160. https://doi.org/10.2514/8.1895

[6] Zhang, Y.-S., Bi, W.-T., Hussain, F., and She, Z.-S., "A Generalized Reynolds Analogy for Compressible Wall-Bounded Turbulent Flows," *Journal of Fluid Mechanics*, Vol. 739, Jan. 2014, pp. 392–420. https://doi.org/10.1017/jfm.2013.620

[7] Chauhan, K., Nagib, H., and Monkewitz, P., "On the Composite Logarithmic Profile in Zero Pressure Gradient Turbulent Boundary Layers," *45th AIAA Aerospace Sciences Meeting and Exhibit*, AIAA Paper 2007-0532, 2007. https://doi.org/10.2514/6.2007-532

[8] Smits, A. J., and Dussauge, J.-P., *Turbulent Shear Layers in Supersonic Flow*, Springer Science & Business Media, New York, 2006, Chap. 7. https://doi.org/10.1007/b137383

[9] Johnson, D. A., and King, L., "A Mathematically Simple Turbulence Closure Model for Attached and Separated Turbulent Boundary Layers," *AIAA Journal*, Vol. 23, No. 11, 1985, pp. 1684–1692. https://doi.org/10.2514/3.9152

[10] Nagib, H. M., and Chauhan, K. A., "Variations of von Kármán Coefficient in Canonical Flows," *Physics of Fluids*, Vol. 20, No. 10, 2008, Paper 101518. https://doi.org/10.1063/1.3006423

[11] Iyer, P. S., and Malik, M. R., "Analysis of the Equilibrium Wall Model for High-Speed Turbulent Flows," *Physical Review Fluids*, Vol. 4, No. 7,

2019, Paper 074604.
https://doi.org/10.1103/PhysRevFluids.4.074604
[12] Coles, D., "The Turbulent Boundary Layer in a Compressible Fluid," RAND Corp. R-403-PR, 1962.
[13] Fernholz, H., and Finleyt, P., "The Incompressible Zero-Pressure-Gradient Turbulent Boundary Layer: An Assessment of the Data," *Progress in Aerospace Sciences*, Vol. 32, No. 4, 1996, pp. 245–311.
https://doi.org/10.1016/0376-0421(95)00007-0
[14] Cebeci, T., and Smith, A. M. O., *Analysis of Turbulent Boundary Layers*, Elsevier, New York, 1974.
[15] Fernholz, H.-H., and Finley, P., "A Critical Commentary on Mean Flow Data for Two-Dimensional Compressible Turbulent Boundary Layers," AGARD AG-253, 1980.
[16] Wenzel, C., Selent, B., Kloker, M., and Rist, U., "DNS of Compressible Turbulent Boundary Layers and Assessment of Data/Scaling-Law Quality," *Journal of Fluid Mechanics*, Vol. 842, May 2018, pp. 428–468.
https://doi.org/10.1017/jfm.2018.179
[17] Bradshaw, P., "Compressible Turbulent Shear Layers," *Annual Review of Fluid Mechanics*, Vol. 9, No. 1, 1977, pp. 33–52.
https://doi.org/10.1146/annurev.fl.09.010177.000341
[18] Trettel, A., and Larsson, J., "Mean Velocity Scaling for Compressible Wall Turbulence with Heat Transfer," *Physics of Fluids*, Vol. 28, No. 2, 2016, Paper 026102.
https://doi.org/10.1063/1.4942022
[19] Spalart, P. R., "Direct Simulation of a Turbulent Boundary Layer Up to $R_\theta = 1410$," *Journal of Fluid Mechanics*, Vol. 187, Feb. 1988, pp. 61–98.
https://doi.org/10.1017/S0022112088000345
[20] Monkewitz, P. A., and Nagib, H. M., "The Hunt for the Kármán 'Constant' Revisited," *Journal of Fluid Mechanics*, Vol. 967, July 2023, Paper A15.
https://doi.org/10.1017/jfm.2023.448
[21] Lee, M., and Moser, R. D., "Direct Numerical Simulation of Turbulent Channel Flow up to $Re_\tau \approx 5200$," *Journal of Fluid Mechanics*, Vol. 774, July 2015, pp. 395–415.
https://doi.org/10.1017/jfm.2015.268
[22] Pirozzoli, S., Romero, J., Fatica, M., Verzicco, R., and Orlandi, P., "One-Point Statistics for Turbulent Pipe Flow up to $Re_\tau \approx 6000$," *Journal of Fluid Mechanics*, Vol. 926, Nov. 2021, Paper A28.
https://doi.org/10.1017/jfm.2021.727
[23] Schlatter, P., Örlü, R., Li, Q., Brethouwer, G., Fransson, J. H., Johansson, A. V., Alfredsson, P. H., and Henningson, D. S., "Turbulent Boundary Layers up to $Re_\theta = 2500$ Studied Through Simulation and Experiment," *Physics of Fluids*, Vol. 21, No. 5, 2009, Paper 051702.
https://doi.org/10.1063/1.3139294
[24] Schlatter, P., and Örlü, R., "Assessment of Direct Numerical Simulation Data of Turbulent Boundary Layers," *Journal of Fluid Mechanics*, Vol. 659, Sept. 2010, pp. 116–126.
https://doi.org/10.1017/S0022112010003113
[25] Jiménez, J., Hoyas, S., Simens, M. P., and Mizuno, Y., "Turbulent Boundary Layers and Channels at Moderate Reynolds Numbers," *Journal of Fluid Mechanics*, Vol. 657, Aug. 2010, pp. 335–360.
https://doi.org/10.1017/S0022112010001370
[26] Sillero, J. A., Jiménez, J., and Moser, R. D., "One-Point Statistics for Turbulent Wall-Bounded Flows at Reynolds Numbers up to $\delta^+ = 2000$," *Physics of Fluids*, Vol. 25, No. 10, 2013, Paper 105102.
https://doi.org/10.1063/1.4823831
[27] Zhang, C., Duan, L., and Choudhari, M. M., "Direct Numerical Simulation Database for Supersonic and Hypersonic Turbulent Boundary Layers," *AIAA Journal*, Vol. 56, No. 11, 2018, pp. 4297–4311.
https://doi.org/10.2514/1.J057296
[28] Bernardini, M., and Pirozzoli, S., "Wall Pressure Fluctuations Beneath Supersonic Turbulent Boundary Layers," *Physics of Fluids*, Vol. 23, No. 8, 2011, Paper 085102.
https://doi.org/10.1063/1.3622773
[29] Cogo, M., Salvadore, F., Picano, F., and Bernardini, M., "Direct Numerical Simulation of Supersonic and Hypersonic Turbulent Boundary Layers at Moderate-High Reynolds Numbers and Isothermal Wall Condition," *Journal of Fluid Mechanics*, Vol. 945, Aug. 2022, Paper A30.
https://doi.org/10.1017/jfm.2022.574
[30] Ceci, A., Palumbo, A., Larsson, J., and Pirozzoli, S., "Numerical Tripping of High-Speed Turbulent Boundary Layers," *Theoretical and Computational Fluid Dynamics*, Vol. 36, No. 6, 2022, pp. 865–886.
https://doi.org/10.1007/s00162-022-00623-0
[31] Nagib, H. M., Chauhan, K. A., and Monkewitz, P. A., "Approach to an Asymptotic State for Zero Pressure Gradient Turbulent Boundary Layers," *Philosophical Transactions of the Royal Society A: Mathematical, Physical and Engineering Sciences*, Vol. 365, No. 1852, 2007, pp. 755–770.
https://doi.org/10.1098/rsta.2006.1948
[32] Pecnik, R., and Hasan, A. M., "Drag and Heat Transfer Estimation," 2023, https://github.com/Fluid-Dynamics-Of-Energy-Systems-Team/DragandHeatTransferEstimation.git.
[33] Huang, J., Nicholson, G. L., Duan, L., Choudhari, M. M., and Bowersox, R. D., "Simulation and Modeling of Cold-Wall Hypersonic Turbulent Boundary Layers on Flat Plate," *AIAA Scitech 2020 Forum*, AIAA Paper 2020-0571, 2020.
https://doi.org/10.2514/6.2020-0571
[34] Griffin, K. P., Fu, L., and Moin, P., "Velocity Transformation for Compressible Wall-Bounded Turbulent Flows with and Without Heat Transfer," *Proceedings of the National Academy of Sciences*, Vol. 118, No. 34, 2021, Paper e2111144118.
https://doi.org/10.1073/pnas.2111144118
[35] Volpiani, P. S., Iyer, P. S., Pirozzoli, S., and Larsson, J., "Data-Driven Compressibility Transformation for Turbulent Wall Layers," *Physical Review Fluids*, Vol. 5, No. 5, 2020, Paper 052602.
https://doi.org/10.1103/PhysRevFluids.5.052602
[36] Patel, A., Boersma, B. J., and Pecnik, R., "The Influence of Near-Wall Density and Viscosity Gradients on Turbulence in Channel Flows," *Journal of Fluid Mechanics*, Vol. 809, 2016, pp. 793–820.
https://doi.org/10.1017/jfm.2016.689
[37] Van Driest, E. R., The Problem of Aerodynamic Heating, *Aerodynamics Aspects Session, National Summer Meeting*, Inst. of the Aeronautical Sciences, Los Angeles, June 1956.
[38] Song, Y., Zhang, P., Liu, Y., and Xia, Z., "Central Mean Temperature Scaling in Compressible Turbulent Channel Flows with Symmetric Isothermal Boundaries," *Physical Review Fluids*, Vol. 7, No. 4, 2022, Paper 044606.
https://doi.org/10.1103/PhysRevFluids.7.044606

P. Durbin
Associate Editor